

Introduction

In a fluidization process, a bed of solid particles acquires fluid-like properties by passing a gas of liquid through it. An efficient bed-to-surface heat transfer and a temperature uniformity are among the major advantages of a gas-fluidized bed reactor, widely used in chemical processing industries, particularly in separation and in catalytic reactions. Its performance, however, depends highly on its hydrodynamics, where solid fraction (α) plays a significant role. Thus, techniques that enable the measurement of α across different sections of the bed are highly important.

The Fluidized bed

In a typical cylindrical fluidized bed, multiple flow patterns can be observed depending upon gas velocity. For low rates of flow, fluid passes through the void space of the particle without disturbing them, thus the bed is fixed. As fluid velocity increases, so does the drag force acting on the particles. At a critical point, the drag force equals the gravitational one (fluidisation point) and the bed fluidises. This process can be represented by Fig.1, where the pressure difference between two points in the bed are plotted against gas velocity.

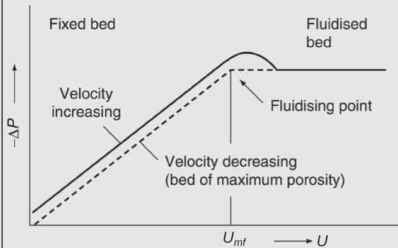


Fig. 2: Reactor bed used in experiments

Fig. 1: Diagram of pressure drop as a function of gas velocity
Source: Chemical Engineering Guides of the University of Florida, 2015

Materials

Aluminium oxide (Al_2O_3) commonly known as Alumina, is used. It has an average particle size of 69 μm . The mean bulk density of the powder is 1068 m^3/kg (2% CV) while its true density is 2900 m^3/kg . A SEM image of Alumina is shown on Fig. 3.

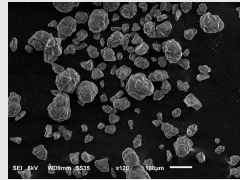


Fig. 3: SEM Image of Alumina

Positron Emission Particle Tracking (PEPT)

PEPT is a non-invasive technique based on the movement of a single tracer particle over a prolonged period of time. A radioactively labelled particle and a pair of positron-sensitive γ -ray detectors are used to locate the particle at a specific time, as shown on Fig. 4. The marker used is generally ^{18}F , ^{61}Cu or ^{66}Ga , which decay via β^+ and hence emit positrons.

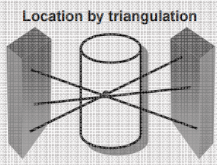


Fig. 4: PEPT Schematic Diagram
Source: Seville, 2010

Experimental Minimum Fluidisation Velocity (u_{mf})

Experimental $u_{mf} = 0.661$ cm/s.
Wen & Wu model predicts $u_{mf} = 0.499$ cm/s (25% error).
Tannaus model predicts $u_{mf} = 0.622$ cm/s (6% error)

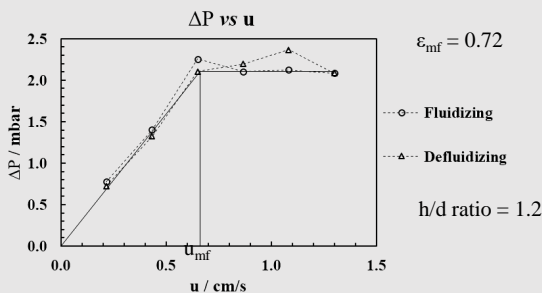


Fig. 5: Experimental Results

Vertical Velocity Profile, Mass Flux and Solid Fraction

Once PEPT data is generated, there are two different methods of determining the bed density ρ_b .

Occupancy Method

Occupancy is defined as the ratio of time the tracer spends in a determined volume over the total time the experiment is conducted. The bed density is then defined as:

$$\rho_b = \frac{occ \times m}{v_{cell}} \quad (I), \text{ where } m \text{ is the total mass of powder and } v_{cell} \text{ the volume of the determined cell.}$$

Mass Flux over velocity Method

The velocity in direction p is calculated using the five-point algorithm, where:

$$\vec{v}_p(i) = 0.1 \left(\frac{\bar{p}_{i+5} - \bar{p}_i}{t_{i+5} - t_i} \right) + 0.15 \left(\frac{\bar{p}_{i+4} - \bar{p}_{i-1}}{t_{i+4} - t_{i-1}} \right) + 0.25 \left(\frac{\bar{p}_{i+3} - \bar{p}_{i-2}}{t_{i+3} - t_{i-2}} \right) + 0.25 \left(\frac{\bar{p}_{i+2} - \bar{p}_{i-3}}{t_{i+2} - t_{i-3}} \right) + 0.15 \left(\frac{\bar{p}_{i+1} - \bar{p}_{i-4}}{t_{i+1} - t_{i-4}} \right) + 0.1 \left(\frac{\bar{p}_i - \bar{p}_{i-5}}{t_i - t_{i-5}} \right)$$

The net mass flux in height i of the j cross-sectional area is defined as:

$$G(i, j) = \frac{m \times (n_1 - n_2)}{S(j) \times t_{total}}, \text{ where } n_1 \text{ and } n_2 \text{ are respectively the number of particles that go upwards and downwards through area } S(j). \text{ The bed density is then } \rho_b = \frac{G(i, j)}{v_{average}(i, j)} \quad (II), \text{ where } v_{average}(i, j) \text{ is an}$$

average of the vertical velocities of particles going through $S(j)$. The bed is divided in 3 levels and in 10 concentric annular rings. Fig. 9, 10 and 11 show radial solid fraction for each level. Fig. 12 and 13 show average velocity and mass flux used for calculating α using (II).

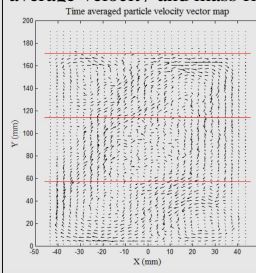


Fig. 6: Time Averaged velocity map across each level

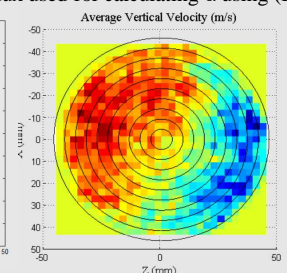


Fig. 7: Time Averaged Vertical Velocity across whole bed height

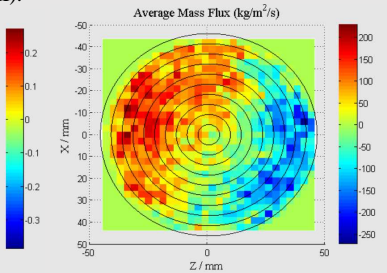


Fig. 8: Time Averaged Mass Flux across whole bed height

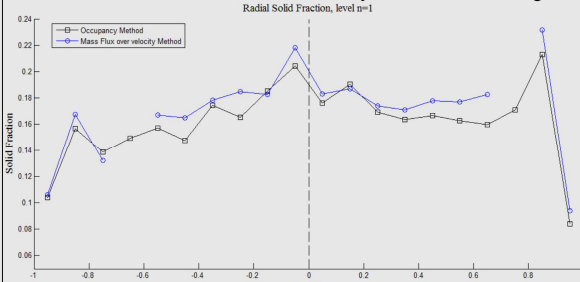


Fig. 9: Radial Solid Fraction at level 1

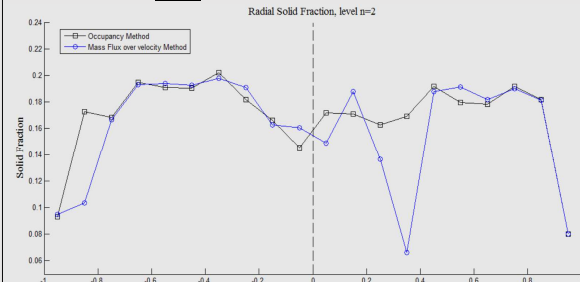


Fig. 10: Radial Solid Fraction at level 2

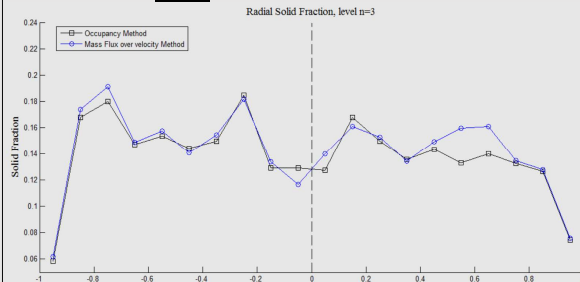


Fig. 11: Radial Solid Fraction at level 3

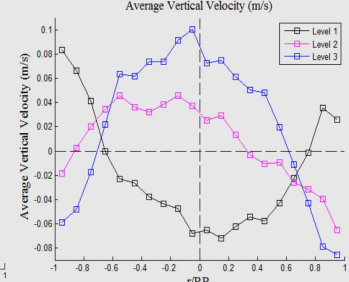


Fig. 12: Radial Time Averaged Velocity

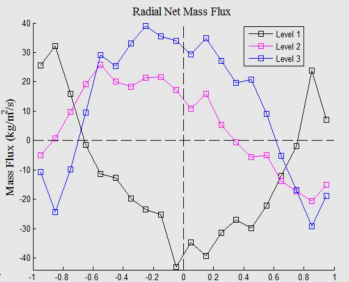


Fig. 13: Radial Time Averaged Mass Flux

- Solid fraction values are within the expected range;
- Symmetry is well observed in levels 3 and 1, whether level 2 show greatest radial asymmetry;
- Two points where inconsistency was found ($\alpha < 0$ or $\alpha > 1$) were omitted.
- Fig. 7 and Fig. 8 show that particles are favourably coming down in one side of the bed and coming up on another side, which is not ideal.

Conclusions

Experimental u_{mf} agrees with model prediction within 10% error. Occupancy method has shown to be more robust and it did not present any inconsistency. Yet, both methods show similar radial- α behaviour, particularly at levels 1 and 3. Results indicate lesser α closer to walls, where particles are moving much faster.

Reference List

Seville, J. A *Single particle view of fluidisation*. The 13th International Conference on Fluidization, Art. 7, 2010
Fluidization: A Unit Operation in Chemical Engineering, University of Florida Chemical Engineering Guides, 2015.

Acknowledgments

Funded by the Brazilian Council for Scientific and Technological Development.
Special acknowledgement to Dr. Pablo Garcia.

